INFECTION AND IMMUNITY, Aug. 2010, p. 3625–3636 Vol. 78, No. 8
0019-9567/10/$12.00 doi:10.1128/IAI.00006-10

Distribution and Phylogeny of Immunoglobulin-Binding Protein G in Shiga Toxin-Producing *Escherichia coli* and Its Association with Adherence Phenotypes▽

Viktor Merkel,[1]# Barbara Ohder,[1]# Martina Bielaszewska,[1] Wenlan Zhang,[1] Angelika Fruth,[2] Christian Menge,[3] Erika Borrmann,[3] Barbara Middendorf,[1] Johannes Müthing,[1] Helge Karch,[1] and Alexander Mellmann[1]*

Institute for Hygiene and Interdisciplinary Center of Clinical Research (IZKF), University of Münster, Robert-Koch-Str. 41, 48149 Münster, Germany[1]; National Reference Center for Salmonella and Other Bacterial Enteric Pathogens, Robert Koch Institute, Branch Wernigerode, Burgstr. 37, 38855 Wernigerode, Germany[2]; and Friedrich-Loeffler-Institut, Institute of Molecular Pathogenesis, Naumburger Str. 96, 07743 Jena, Germany[3]

Received 6 January 2010/Returned for modification 6 February 2010/Accepted 30 May 2010

eibG* in Shiga toxin-producing *Escherichia coli* (STEC) O91 encodes a protein (EibG) which binds human immunoglobulins G and A and contributes to bacterial chain-like adherence to human epithelial cells. We investigated the prevalence of *eibG* among STEC, the phylogeny of *eibG*, and *eibG* allelic variations and their impact on the adherence phenotype. *eibG* was found in 15.0% of 240 *eae*-negative STEC strains but in none of 157 *eae*-positive STEC strains. The 36 *eibG*-positive STEC strains belonged to 14 serotypes and to eight multilocus sequence types (STs), with serotype O91:H14/H$^-$ and ST33 being the most common. Sequences of the complete *eibG* gene (1,527 bp in size) from *eibG*-positive STEC resulted in 21 different alleles with 88.11% to 100% identity to the previously reported *eibG* sequence; they clustered into three *eibG* subtypes (*eibG*-α, *eibG*-β, and *eibG*-γ). Strains expressing EibG-α and EibG-β displayed a mostly typical chain-like adherence pattern (CLAP), with formation of long chains on both human and bovine intestinal epithelial cells, whereas strains with EibG-γ adhered in short chains, a pattern we termed atypical CLAP. The same adherence phenotypes were displayed by *E. coli* BL21(DE3) clones containing the respective *eibG*-α, *eibG*-β, and *eibG*-γ subtypes. We propose two possible evolutionary scenarios for *eibG* in STEC: a clonal development of *eibG* in strains with the same phylogenetic background or horizontal transfer of *eibG* between phylogenetically unrelated STEC strains.

Shiga toxin (Stx)-producing *Escherichia coli* (STEC) causes diarrhea, bloody diarrhea, and the hemolytic uremic syndrome (HUS), the most common cause of acute renal failure in children (15, 36). Besides expressing Stx, most STEC strains from patients cause the attaching-and-effacing lesions in host cells, a phenotype mediated by intimin (encoded by *eae*) and other proteins encoded on the locus of enterocyte effacement (LEE) pathogenicity island (7, 14). STEC O157:H7, the globally predominant and best-studied STEC strain, possesses *eae* (15), but a subset of STEC strains associated with human disease lack *eae*; among these, strains of serogroup O91 are the most common (2, 4, 13, 39, 40).

A group of immunoglobulin-binding proteins was first found (28, 29) in the *E. coli* standard collection of reference (ECOR), which consists of 72 natural *E. coli* isolates from humans and other mammals (22). EibA, EibC, EibD, and EibE are synthesized by ECOR-9 (29), and an additional protein, EibF, is expressed by ECOR-2 (30). A recently described member of the Eib family, EibG, was detected in STEC O91 but not in STEC O26, O111, and O157 (17). The *E. coli* O91 EibG protein has dual roles: it binds, by nonimmune mechanisms, human IgG and IgA and also participates in bacterial adherence to host epithelial cells (17). The *E. coli* O91 strains harboring the *eibG* gene display chain-like adherence to cultured epithelial cells, which was also observed in *E. coli* laboratory strains possessing cloned *eibG* (17). *E. coli* O91 strains, in which a transposon has interrupted *eibG*, lose their chain-like adherence pattern (CLAP), indicating that EibG contributes to this adherence phenotype. However, the distribution of this nonfimbrial adhesin within a broad spectrum of STEC serotypes is unknown. Therefore, we determined the prevalence of *eibG* in a large collection of STEC strains and analyzed allelic variations in this gene and their correlation with the CLAP phenotype. Moreover, we investigated the relationships between the different alleles of *eibG* and their host strains by comparing the phylogenetic tree of *eibG* with the multilocus sequence typing (MLST) profiles.

MATERIALS AND METHODS

Strains and their characterization. We sought to determine the frequency of *eibG* in 157 *eae*-positive and 240 *eae*-negative STEC strains belonging to 104 serotypes (Table 1). These strains were isolated between 1995 and 2008 from patients with diarrhea and/or HUS and from asymptomatic carriers (all together, 391 strains) and environmental samples (cattle feces, water, and food) (six strains) at the Institute for Hygiene, University of Münster, Münster, Germany, and at the Robert Koch Institute, Wernigerode, Germany (4, 12, 20). The rationale behind this collection, which is a subset of our institutional strain collection, was that we randomly chose up to four strains per serotype per year

* Corresponding author. Mailing address: Institut für Hygiene, Universitätsklinikum Münster, Robert-Koch-Str. 41, 48149 Münster, Germany. Phone: 49 251 83 52316. Fax: 49 251 83 55341. E-mail: mellmann@uni-muenster.de.

# Both authors contributed equally.

▽ Published ahead of print on 14 June 2010.

TABLE 1. Distribution of *eibG* among *eae*-positive and *eae*-negative STEC

eae status	No. of strains tested	No. (%) of *eibG*-positive strains	Serotype (no. of tested strains)[a]
Positive	157	0	O26:H11/H$^-$ (53), O103:H2/H$^-$ (13), O111:H8/H$^-$ (14), O121:H19 (1), O145:H25/28/H$^-$ (25), O157:H7/H$^-$ (NSF) (40), O157:H$^-$ (SF) (6), Ont:H18/H$^-$ (2), OR:H11 (1), OR:H$^-$ (2)
Negative	240	36 (15.0)	O1:H10/Hnt (2), O3:H2 (1), O3:H10 (1), O5:H$^-$ (5), O6:H$^-$ (1), O6:Hnt (2), O8:H$^-$ (4), O8:H10 (2), O8:H14 (1), O8:H19 (1), O8:Hnt (2), O15:H21 (1), O22:H8 (7), O23:H15 (2), O23:H19 (1), O40:H8 (4), O41:H$^-$ (1), O55:Hnt (1), O68:H4 (1), O74:H42 (2), O75:H8/H21 (2), O76:H19 (4), O78:H$^-$ (3), O86:H$^-$ (2), O91:H8 (1), O91:H10 (2), O91:H14/H$^-$/Hnt[b] (22), O91:H21 (19), O104:H16 (1), O104:H21 (1), O106:H18 (2), O112:H2 (1), O113:H4 (10), O113:H21 (4), O115:H$^-$ (2), O116:H21 (1), O118:H12 (1), O128:H2 (10), O128:H$^-$ (3), O146:H$^-$ (2), O146:H8 (2), O146:H21 (2), O146:H28 (6), O146:H31 (1), O146:H51 (1), O152:H$^-$ (2), O152:H4 (1), O153:H18 (3), O153:H25 (1), O154:H20/H31/Hnt (3), O163:H19 (2), O168:H8 (1), O174:H$^-$ (1), O174:H2 (4), O174:H8 (3), O174:H21 (1), O175:H16 (2), O175:H28 (1), O176:H$^-$ (1), O178:H$^-$ (3), O178:H8 (2), O178:H19 (5), O181:H16 (2), O181:H49 (1), Ont:H$^-$ (14), Ont:H2/H4/H10/H14/H19 (5), Ont:H18 (3), Ont:H21 (4), Ont:H28 (2), Ont:H30 (1), Ont:Hnt (1), OR:H$^-$ (8), OR:H2 (2), OR:H10/H14 (2), OR:H21 (6), OR:H45 (2), OR:Hnt (3)

[a] H$^-$, nonmotile; OR (Orough), autoagglutinable strains; Ont, O nontypeable; Hnt, H nontypeable.
[b] All strains possess *fliC*$_{H14}$.

to ensure that the collection is not biased by epidemiologically related isolates. In addition to the above strains, the presence of *eibG* was sought in 42 reference STEC strains representing all serotypes associated with HUS in Germany ("the HUSEC collection") (19) and in the ECOR collection (22) (kindly provided by T. Whittam, deceased, National Food Safety & Toxicology Center, Michigan State University).

Characterization of isolates. The isolates were confirmed as *E. coli* using the API 20 E test kit (bioMérieux, Marcy l'Etoile, France) and serotyped (26). In nonmotile isolates of serogroup O91, the presence of the *fliC* gene encoding the flagellar subunit of the H14 antigen was sought using PCR restriction fragment-length polymorphism (RFLP) (5). If appropriate, the presence of the gene cluster encoding biosynthesis of the O91 antigen was determined using PCR targeting *wzy*$_{O91}$ (25).

Detection and sequence analysis of *eibG*. To detect *eibG*, we used the PCR strategy described by Lu et al. (17), which applies a primer pair, 1114orf1Fp (5′-ATCGGCTTTCATCGCATCAGGAC-3′) and 1114orf1Rp (5′-CCACAAG GCGGGTATTCGTATC-3′), located within the *eibG* gene. Briefly, 10 pmol of the primers 1114orf1Fp and 1114orf1Rp was used in a 25-μl PCR mixture containing 12.5 μl Red *Taq* Ready mix (Sigma-Aldrich, Munich, Germany) and 20 ng of chromosomal DNA. PCRs were carried out in a T1 thermocycler (Biometra, Göttingen, Germany) and consisted of an initial denaturation (10 min at 95°C) followed by 35 cycles of denaturation (30 s at 94°C), annealing (60 s at 57°C), and extension (60 s at 72°C) and a final extension (10 min at 72°C). For all isolates that were positive in this PCR, we attempted to sequence the complete gene. To this end, we first used the primers covering the whole *eibG* gene published by Lu et al. (orf1Fw and orf1Rw) to generate the sequencing template using the same conditions described previously (17). In addition, we designed further primers (orf1FWa [5′-GGCGACAAAGATATTGAGATG-3′], eibG_3305f [5′-TTTCGGAATATCCTGAATAAAGCCG-3′], eibG_3902r [5′-CGCCGCACTAGCCTGAAC-3′], eibG_4342f [5′-GATGCTGCAACCGTTC GTCAG-3′], eibG_4889r [5′-TTAAAACTCGAAGTTAACGCC-3′], eibG_ 4919r [5′-GCCGTCATGCTTCATGTCAC-3′], eibG_3380f [5′-CAGATAATT TAACAGGATATCCA-3′]), located on different positions within *eibG*, to achieve a 2-fold sequence coverage over the complete gene. For sequencing, the double-stranded PCR product was purified enzymatically using exonuclease I (New England Biolabs GmbH, Frankfurt-Hoechst, Germany) and shrimp alkaline phosphatase (USB Amersham, Freiburg, Germany), modified from the method of Dugan et al. (9). Briefly, 5 μl of the PCR product was incubated with 1 U of each enzyme at 37°C for 45 min prior to enzyme inactivation at 80°C for 15 min, and the PCR products were stored at 4°C. The purified amplicons were sequenced using the ABI Prism BigDye Terminator v3.1 ready reaction cycle sequencing kit (Applied Biosystems, Foster City, CA), using 0.5 μl of premix from the kit, 1.8 μl Tris-HCl-$MgCl_2$ buffer (400 mM Tris-HCl; 10 mM $MgCl_2$), 10 pmol of sequencing primer (the same as PCR primers), and 2 μl of the PCR product in a total volume of 10 μl. The resulting sequence trace files were assembled and further analyzed using the Ridom Seqsphere software program, version 0.9 beta (Ridom GmbH, Würzburg, Germany) and compared to the *eibG* reference sequence (GenBank accession no. AB255744). Alleles were numbered randomly starting from 001 (*eibG* reference sequence). The codon-based test of neutrality for analysis between the different allelic sequences was performed using the MEGA software program, version 4.0, with default analysis values (34), calculating the probability of rejecting the null hypothesis of strict neutrality, i.e., the number of nonsynonymous substitutions per nonsynonymous sites (d_N) equals the number of synonymous substitutions per synonymous sites (d_S). In

TABLE 2. Clones harboring different *eibG* subtypes from STEC strains

Clone designation	Parental STEC strain				
	Strain no.	Serotype[a]	ST[b]	*eibG* subtype	CLAP[c]
B-1-10	1809/00	O91:H14	33	α	Long chains (typical)
B-10-9	4789/97-1	O146:H21	442	α	Short chains, clusters, single bacteria (atypical)
B-20-1	06-03233	O152:H$^-$ [H14]	13	β	Long chains (typical)
B-18-2	0520/99	Ont:H30	753	γ	Short chains, often parallel (atypical)

[a] Ont, O-antigen nontypeable; H$^-$ [H14], nonmotile strain containing *fliC*$_{H14}$.
[b] ST, sequence type.
[c] CLAP, chain-like adherence pattern.

TABLE 3. Serotypes and sequence types of the 36 *eibG*-positive strains

Strain no.	Serotype[a]	Sequence type	*eibG* allele (GenBank accession no.)	% identity to reference sequence (1,527 bp)[b]
06-03233	O152:H$^-$ [H14]	13	020 (HM236821)	90.39
06-03229	O152:H$^-$ [H14]	13	NA[c]	NA
1809/00	O91:H14 [H14]	33	001 (AB255744)	100
06-08452	O91:H$^-$ [H14]	33	001 (AB255744)	100
27358/97	O91:H14 [H14]	33	001 (AB255744)	100
4308/98	O91:H14 [H14]	33	001 (AB255744)	100
3558/96	Ont:H$^-$[d] [H14]	33	001 (AB255744)	100
7140/96	O91:H$^-$ [H14]	33	003 (GU295803)	99.87
6705/95	OR:H14[d] [H14]	33	004 (GU295804)	99.87
07-00349	O91:H$^-$ [H14]	33	005 (GU295805)	99.08
172/98	OR:H$^-$[d] [H14]	33	005 (GU295805)	99.08
01/E243	O91:H$^-$ [H14]	33	006 (GU295806)	99.87
02-03777	O91:H$^-$ [H14]	33	007 (GU295807)	99.87
07-00739	O91:H$^-$ [H14]	33	008 (GU295808)	99.02
4792/97	O91:H$^-$ [H14]	33	009 (GU295809)	99.87
6561/95	Ont:H$^-$[d] [H14]	33	010 (GU295810)	98.89
07-00740	O91:H$^-$ [H14]	33	011 (GU295811)	99.87
02-03884	O91:H$^-$ [H14]	33	012 (GU295812)	99.02
393/98	O91:H$^-$ [H14]	33	013 (GU295813)	99.93
4798/97	O91:Hnt [H14]	33	013 (GU295813)	99.93
02-07123	O91:H$^-$ [H14]	33	013 (GU295813)	99.93
4884/97	OR:Hnt[d] [H14]	33	015 (HM236816)	99.02
2875/96	O91:H14 [H14]	33	016 (HM236817)	99.93
3671/97	O91:H$^-$ [H14]	33	017 (HM236818)	99.08
4789/97-1	O146:H21	442	015 (HM236816)	99.02
4141/96	OR:H21[e]	442	NA	NA
4831/97	OR:H45	656	014 (HM236815)	99.87
6451/98	OR:H45	656	014 (HM236815)	99.87
0550/01	O91:H14 [H14]	690	018 (HM236819)	99.93
06-07635	O91:H14 [H14]	690	018 (HM236819)	99.93
06-07349	O91:H14 [H14]	690	019 (HM236820)	99.80
ST234	O146:H28	738	NA	NA
ST295/1	O146:H28	738	NA	NA
99-02787	OR:H10[e]	745	002 (GU295802)	99.87
0519/99	OR:Hnt	753	021 (HM236822)	88.11
0520/99	Ont:H30	753	021 (HM236822)	88.11

[a] [H14], the strains possess *fliC*$_{H14}$.
[b] GenBank accession number AB255744.
[c] NA, not applicable because of amplification failure using various primers covering the complete *eibG* gene, resulting in either a partial *eibG* sequence, which includes only approximately 1 kb of the 3′ end of *eibG* (strains ST234 and ST295/1), or in ambiguous sequences, probably because of different copies of the gene (strains 06-03229 and 4141/96).
[d] The strains possess the O91 biosynthetic cluster, as indicated by a positive result in PCR targeting *wzy*$_{O91}$ (24).
[e] The strains lack the O91 biosynthetic cluster, as indicated by a negative result in PCR targeting *wzy*$_{O91}$.

addition to selection analysis, recombination analysis among all *eibG* alleles and among all *eibG*-positive sequence types (STs) was carried out by using the GENECONV algorithm within the Recombination Detection Program software, v. 3 beta 42 (18). Construction of neighbor-joining trees and calculation of bootstrap values were also performed using the MEGA software program. Using the topology only of trees based on concatenated MLST gene sequences and complete *eibG* sequences, the tanglegram was constructed manually to display the correlation between the MLST sequence type and the *eibG* allele.

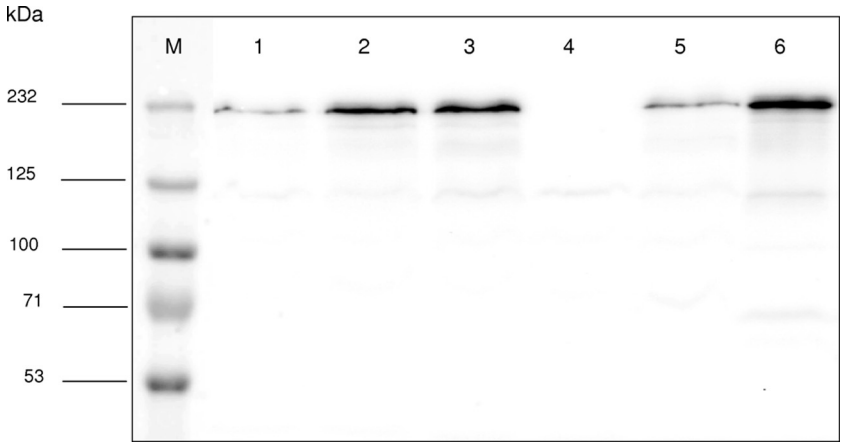

FIG. 1. Expression of EibG in STEC O91, as demonstrated by Western blotting of STEC O91 cell lysates with HRP-conjugated human IgG Fc fragment. In lanes 1 to 6, the following strains (STs are in parentheses) are shown: lane 1, O91:H14 (ST33); lane 2, Ont:H$^-$ [*wzy*$_{O91}$+, *fliC*$_{H14}$] (ST33); lane 3, O91:H$^-$ [*fliC*$_{H14}$] (ST33); lane 4, O91:H21 (ST442) (negative control); lane 5, O91:Hnt [*fliC*$_{H14}$] (ST33); and lane 6, OR:Hnt [*wzy*$_{O91}$+, *fliC*$_{H14}$] (ST33); lane M, molecular mass marker.

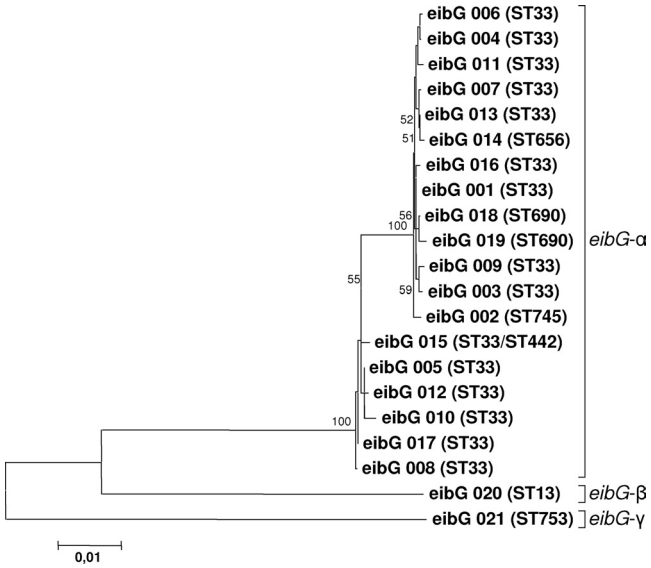

FIG. 2. Unrooted neighbor-joining tree of all 21 unique *eibG* alleles based on complete (1,527 bp) *eibG* sequences, illustrating their phylogenetic relationships and grouping them into three subtypes (*eibG*-α, *eibG*-β, and *eibG*-γ). Bootstrap values (values > 50% are shown) using 1,000 replicates are displayed on the corresponding branches. In parentheses, the related STs for each *eibG* allele are given.

***eibG* cloning.** The *eibG* clones and the STEC strains used as sources of the different *eibG* alleles are listed in Table 2. The complete *eibG* genes from strains 1809/00 and 06-03233 were amplified with the primer pair orf1Fw and orf1Rw (17) and those from strains 4789/97-1 and 0520/99 with primer pair eibG_3305f and orf1Rw. The amplification was performed using the high-fidelity DNA polymerase Phusion Hot Start II (Finnzymes, Espoo, Finland) in 34 cycles of denaturing (94°C, 30 s), annealing (60°C, 60 s), and extension (72°C, 150 s). The PCR products were purified using the QIAQuick PCR purification kit (Qiagen, Hilden Germany) and ligated into the pGEM-T Easy vector (Promega, Mannheim, Germany) according to the manufacturer's instructions. The constructs were transformed into *E. coli* BL21(DE3) chemically competent cells (Stratagene Europe, Amsterdam, Netherlands) using the heat shock method. The clones were selected on LB agar containing ampicillin (100 μg/ml), X-Gal (5-bromo-4-chloro-3-indolyl-β-D-galactopyranoside) (40 μg/ml) and IPTG (isopropyl-β-D-thiogalactosylpyranoside) (1 mM). The correct orientation of the *eibG* inserts in the clones and the correct sequence of the inserts were verified by sequencing using the primers M13f (5′-TGTAAAACGACGGCCAGT-3′) and M13r (5′-CAGGAAACAGCTATGACC-3′) and the above-mentioned primers for complete sequencing to achieve a 2-fold sequence coverage.

MLST. MLST of *eibG*-positive strains was performed as described previously (19), and allelic sequences were deposited at the MLST website (http://mlst.ucc.ie/mlst/dbs/Ecoli). The minimum spanning tree was constructed using the Ridom Seqsphere software program, version 0.9 beta (Ridom GmbH).

Protein immunoblotting. Bacterial overnight cultures in Luria-Bertani (LB) broth were pelleted by centrifugation (5,000 × *g*, 20 min), heat lysed (99°C, 10 min) in SDS-PAGE sample buffer, and separated by SDS-PAGE under reducing conditions using 8% separating gels (Mini Protean 3 cell system; Bio-Rad GmbH, Munich, Germany). SDS-PAGE-separated proteins were transferred on a polyvinylidene difluoride (PVDF) membrane (Whatman GmbH, Dassel, Germany) using a semidry blotting system (V20-SBD; Roth, Karlsruhe, Germany). The membrane was blocked for 1 h in 5% (wt/vol) skim milk in Tris-buffered saline (TBS) (pH 7.5) supplemented with 0.05% (vol/vol) Tween 20 (TBS-T) and then incubated for 12 h with horseradish peroxidase (HRP)-conjugated human IgG Fc fragment (100 ng/ml) (Jackson ImmunoResearch Laboratories, Inc., West Grove, PA). After incubation with substrate solution (SuperSignal West Pico chemiluminescent substrate; Pierce Biotechnology, Rockford, IL), bound Fc fragments were detected using a chemiluminescence photoimager (Bio-Rad GmbH).

Fluorescence microscopy. Overnight cultures of STEC strains in LB broth or of EibG clones in LB broth with ampicillin (100 μg/ml) and induced with IPTG (2 h, 37°C) (~1×10^8 CFU in 300 μl) were added to wells of 4-well Permanox Lab-Tek chamber slides (Nunc GmbH, Langenselbold, Germany) and allowed to adhere to the surface for 18 h. The slides were washed with phosphate-buffered saline (PBS) and fixed with 70% ethanol (5 min at room temperature). After blocking with 5% (wt/vol) bovine serum albumin (BSA) and 0.2% (wt/vol) fish skin gelatin (Sigma-Aldrich) in PBS (2 h at room temperature), Alexa 488-conjugated human IgG Fc fragment (DyLight 488 ChromPure human IgG Fc

TABLE 4. Association between *eibG* allele and chain-like adherence phenotype

Strain no.	Serotype[a]	Sequence type	*eibG* allele	*eibG* subtype[b]	% nucleotide identity to reference sequence (no. of point mutations, synonymous/nonsynonymous)	Predominant adherence phenotype (HCT-8)[c]
1809/00	O91:H14 [H14]	33	001	α	100.00 (0/0)	Long chains
3558/98	Ont:H$^-$ [H14]	33	001	α	100.00 (0/0)	Long chains
7140/96	O91:H$^-$ [H14]	33	003	α	99.87 (0/2)	Long chains
07-00349	O91:H$^-$ [H14]	33	005	α	99.08 (6/8)	Long chains
02-03777	O91:H$^-$ [H14]	33	007	α	99.87 (0/2)	Long chains
07-00739	O91:H$^-$ [H14]	33	008	α	99.02 (6/9)	Long chains
4792/97	OR:H$^-$ [H14]	33	009	α	99.87 (1/1)	Long chains
07-00740	O91:H$^-$ [H14]	33	011	α	99.87 (0/2)	Long chains
02-03884	O91:H$^-$ [H14]	33	012	α	99.02 (7/8)	Long chains
3671/97	O91:H$^-$ [H14]	33	017	α	99.08 (6/8)	Long chains
4789/97-1	O146:H21	442	015	α	99.02 (6/9)	Short chains, small clusters, and single bacteria
4831/97	OR:H45	656	014	α	99.87 (0/2)	Short chains, small clusters, and single bacteria
0550/01	O91:H14 [H14]	690	018	α	99.93 (0/1)	Long chains
06-07349	O91:H14 [H14]	690	019	α	99.80 (0/3)	Long chains
99-02787	OR:H10[d]	745	002	α	99.87 (1/1)	Long chains
06-03233	O152:H$^-$ [H14]	13	020	β	90.39 (61/86)	Long chains
0519/99	OR:Hnt	753	021	γ	88.11 (78/106)	Short chains, small clusters
0520/99	Ont:H30	753	021	γ	88.11 (78/106)	Short chains, often parallel

[a] [H14], the strains possess $fliC_{H14}$; strains 4792/97 (OR:H$^-$) and 3558/98 (Ont:H$^-$) harbor the O91 antigen biosynthetic cluster.
[b] *eibG* subtypes β and γ differ from the *eibG* reference sequence (*eibG* subtype α; GenBank accession number AB255744) by at least 2% on the nucleotide level and have a sequence similarity of ≤98% to any other subtype.
[c] Chains classified as long contain more than 10 (usually ca. 15) bacteria, and chains classified as short contain less than 10 bacteria.
[d] The strains lack the O91 biosynthetic cluster, as indicated by a negative result in PCR targeting wzy_{O91}.

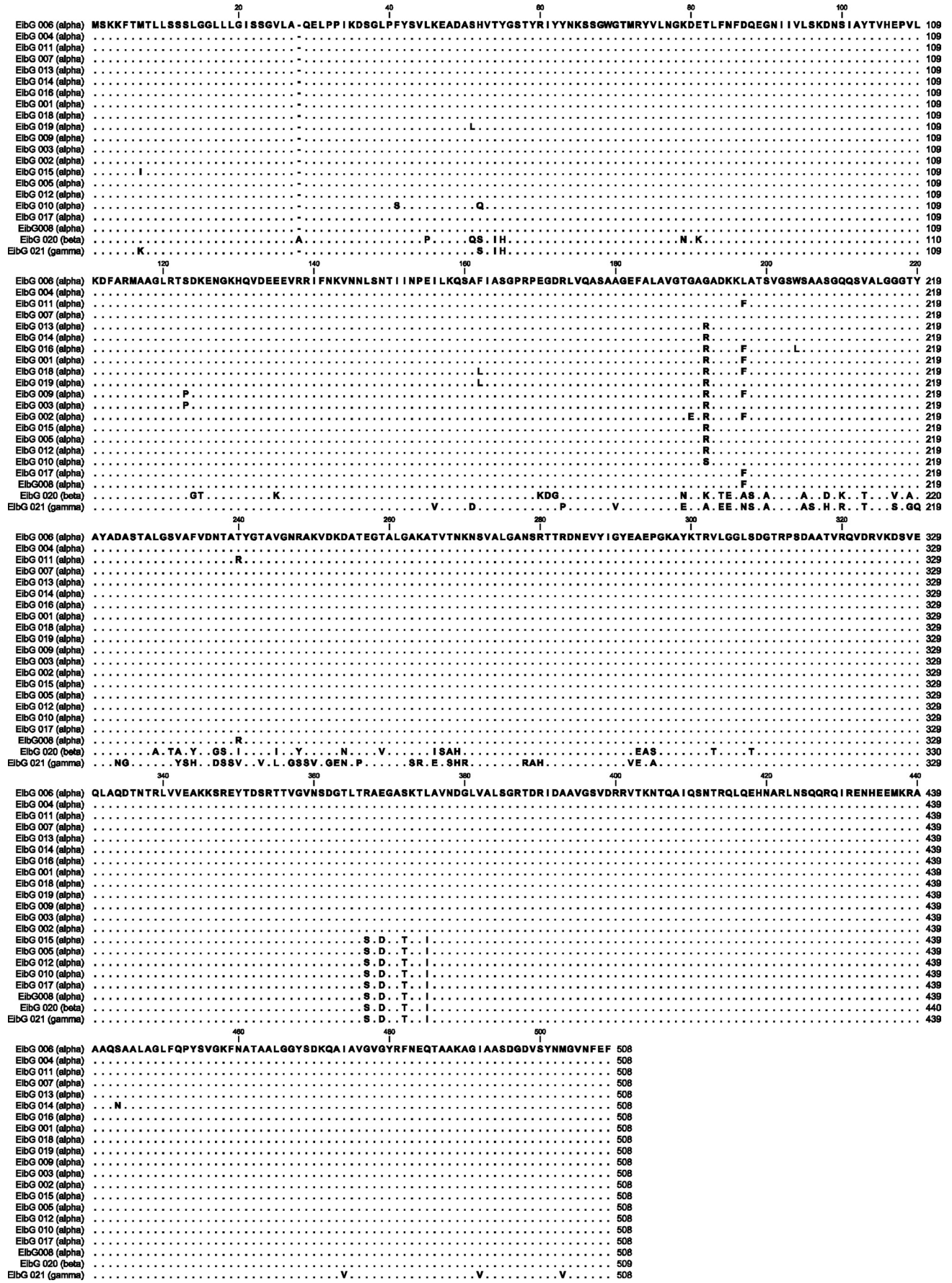

FIG. 3. Protein alignment of the 21 EibG alleles predicted from their nucleotide sequences in comparison to the reference sequence (EibG 001).

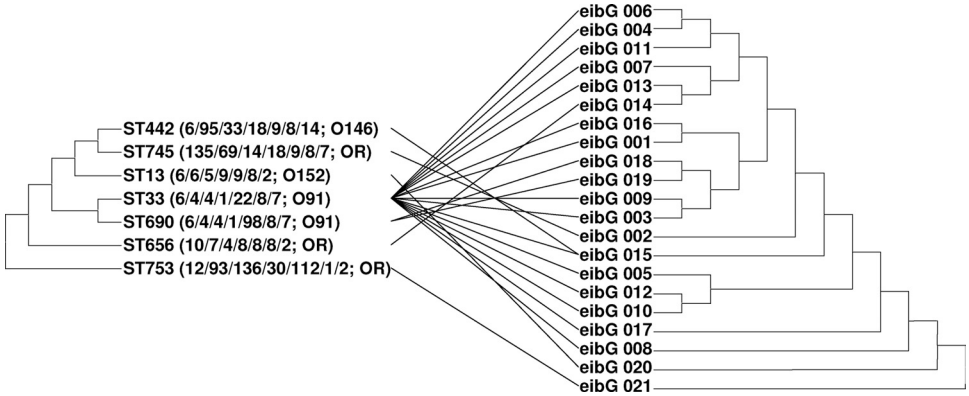

FIG. 4. Tanglegram based on the topology of neighbor-joining trees of the concatenated MLST gene sequences (3,423 bp) and of complete *eibG* gene sequences (1,527 bp). In parentheses, the allelic profiles of each ST and the corresponding serogroups (OR [Orough], autoagglutinable strains) are given. The tanglegram illustrates the association between the genomic background (represented by MLST data) and the different *eibG* alleles showing either clonal diversification of *eibG* within the same genomic background (e.g., *eibG* 018 and 019 within ST690, serogroup O91) or possible horizontal gene transfer of *eibG* between different genomic backgrounds (e.g., *eibG* 015 in ST33, serogroup O91, and in ST442, serogroup O146).

fragment; Jackson ImmunoResearch Laboratories) diluted 1:500 in PBS with 1% BSA was added, and slides were incubated for 2 h at room temperature. After washing, slides were stained with DAPI (4′,6-diamidino-2-phenylindole) (Sigma-Aldrich) diluted 1:1,000 in PBS (15 min at room temperature), mounted in an antifade mounting medium (Dianova, Hamburg, Germany), and examined by a fluorescence microscope (Axio Imager.A1, Zeiss, Jena, Germany). In some experiments, bacteria fixed on the Permanox slides had been preincubated (overnight at room temperature, with gentle shaking) with unconjugated human IgG Fc fragment (diluted 1:500 in PBS with 1% BSA) before they were stained with the Alexa 488-conjugated human IgG Fc fragment.

Cell cultures and CLAP assay. The human intestinal epithelial cell line HCT-8 (human ileocecal adenocarcinoma epithelial cells; ATCC CCL-244) was cultured as described previously (1, 33). The bovine fetal intestinal jejunal epithelial cell line FKD-R 971 was generated by Roland Riebe (RIE 971, collection of cell lines in veterinary medicine; Friedrich-Loeffler-Institut, Federal Research Institute for Animal Health, Greifswald Insel Riems, Germany). Immunohistochemistry using cross-reactive anti-human cytokeratin type II antibody (clone MCA888H; AbD Serotec, Düsseldorf, Germany) and mouse antivimentin antibody (clone V9; Sigma-Aldrich, Taufkirchen, Germany) revealed a moderate staining of FKD-R 971 for both markers. However, the cells showed a characteristic cytoplasmic network of cytokeratin fibers characteristic of epithelial cells. Recent work of our group proved that primary bovine intestinal epithelial cells rapidly upregulate vimentin upon *in vitro* culture (6). Hence, we consider FKD-R 971 to be of epithelial origin. The FKD-R 971 cells were maintained in Dulbecco's modified Eagle medium (DMEM) F-12 medium (Lonza, Cologne, Germany) supplemented with 10% fetal calf serum (FCS) (PAA, Pasching, Austria) at 37°C in a 5% CO_2 atmosphere.

For the adherence assay, HCT-8 cells (2×10^5 per well) and FKD-R 971 cells (1×10^5 per well) were seeded, in antibiotic-free medium, into 4-well glass Lab-Tek chamber slides (Nunc) and grown (37°C, 5% CO_2) until approximately 70% confluence. The monolayers were washed three times with FCS-free medium, infected with 100 μl of overnight (16 h, 37°C, 180 rpm) bacterial cultures diluted 1:20 in FCS-free medium (~1×10^8 CFU), and incubated with or without 0.5% (wt/vol) D-mannose (Roth) in the cell culture medium for 4 h. The cells were then extensively washed with PBS, fixed with 70% ethanol, stained with 10% Giemsa stain (Merck, Darmstadt, Germany), and examined by light microscopy (Axio Imager.A1; Zeiss).

The adherence of *eibG* clones was tested as described above except that the strains were grown (16 h, 37°C, 180 rpm) in LB broth supplemented with ampicillin (100 μg/ml) and expression of EibG was induced using 1 mM IPTG (2 h, 37°C).

Nucleotide sequence accession numbers. Newly determined *eibG* allelic sequences have been deposited in GenBank (accession no. GU295802 to GU295813 and HM236815 to HM236822).

RESULTS

Distribution of *eibG* among STEC strains. *eibG* was found in 36 of 240 (15.0%) *eae*-negative STEC strains but in none of the 157 *eae*-positive STEC strains (Table 1). Of particular interest are strains of serogroup O91, where *eibG* was originally identified (17). *eibG* is present only in strains of serotype O91:H14/H^-/Hnt [H14] (designates strains harboring $fliC_{H14}$), not in those of serotypes O91:H21, O91:H8, and O91:H10 (Tables 1 and 3). EibG expression in STEC O91:H14/H^- [H14] strains is demonstrated in Fig. 1. Only 1 of 42 strains in the HUSEC collection (HUSEC028, serotype O128:H2) produced a weak signal in the *eibG* PCR (17); the remainder were negative. Interestingly, the same phenotype was observed in two other (non-HUSEC) strains of serotype O128:H2. None of the 72 strains of the ECOR collection produced an amplicon in the *eibG* PCR used.

Allelic variations of *eibG*. To determine the allelic variation within *eibG*, we tried to sequence the complete *eibG* genes from all 39 isolates that were positive in the PCR detection assay. Since the sequences of the three O128:H2 strains exhibited a 528-bp deletion in comparison to the *eibG* reference sequence and showed a higher sequence similarity to *eibE* (92.8%) than to *eibG* (90.4%), we excluded these three strains from further analysis. For 32 of the remaining 36 isolates, we were able to sequence the complete *eibG* genes. For the remaining four isolates, either no amplification of the whole gene occurred, probably because of deletions in the 5′ region (strains ST234 and ST295/1), or sequences were ambiguous, probably because of different copies of the gene (strains 06-03229 and 4141/96). Therefore, we also excluded these strains from further analysis. Table 3 summarizes the sequencing results and also displays the serotypes and STs of the 36 *eibG*-positive STEC strains. Complete *eibG* sequencing (1,527 bp) resulted in 21 different *eibG* alleles, with sequence similarities to the reference sequence (GenBank accession number AB255744) (allele *eibG* 001) ranging from 88.11% to 100%. This further enabled us to cluster the different alleles into three *eibG* subtypes (*eibG*-α, *eibG*-β, and *eibG*-γ) (Fig. 2).

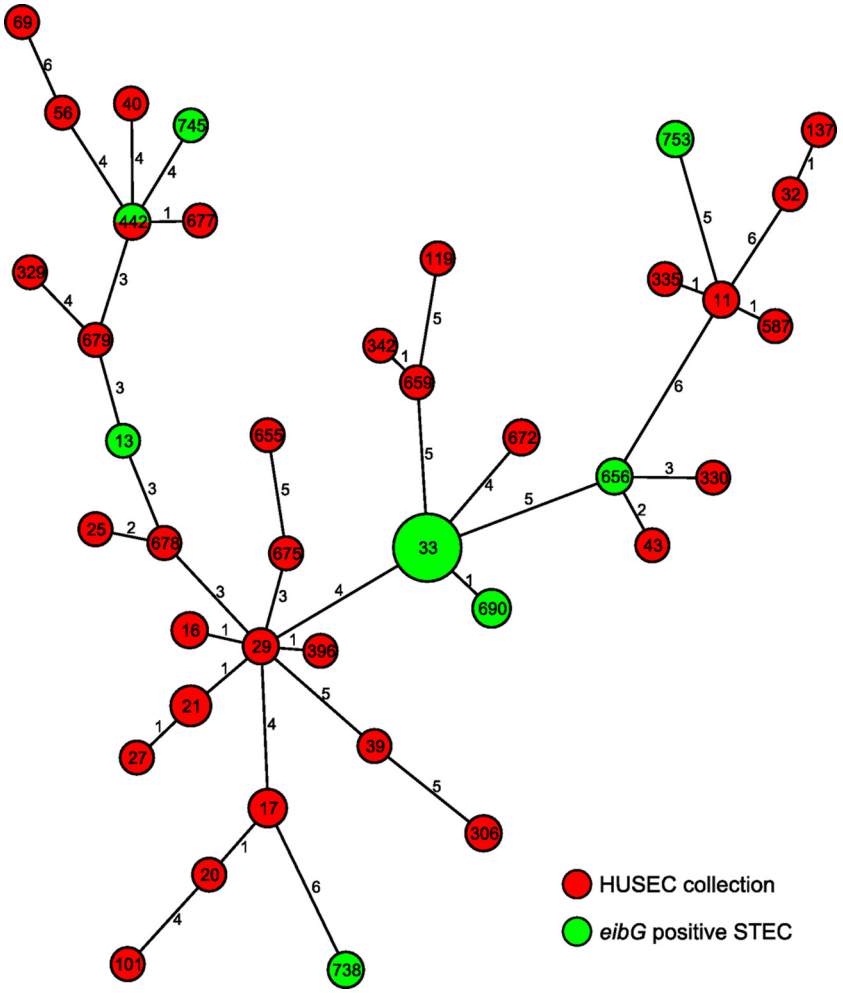

FIG. 5. Minimum spanning tree based on the MLST allelic profiles, portraying the clonal distribution of the *eibG*-positive STEC strains in comparison to the HUSEC collection. Each dot represents a given sequence type (ST), and the size of the circle is proportional to the number of strains analyzed. Connecting lines of increasing length illustrate, and numbers on these lines indicate, the number of alleles that are different between two STs.

Interestingly, all alleles differing from the reference sequence (allele *eibG* 001) had at least one nonsynonymous base exchange (Table 4). Moreover, with two exceptions only (eibG 002 and 009), which had one synonymous and one nonsynonymous base exchange each, all alleles had sustained more nonsynonymous than synonymous base exchanges. Figure 3 illustrates the consequences on the amino acid level as a multiple alignment of all unique alleles. Investigation of the probability of rejecting the null hypothesis ($d_N = d_S$), i.e., no statistically significant presence of either positive selection or purifying selection, found statistical significance not only within all alleles of *eibG*-α but also over all *eibG* alleles. Analysis of recombination events using the GENCONV algorithm (Department of Mathematics, Washington University [http://www.math.wustl.edu/~sawyer/]) resulted in a highly variable *eibG* region from base position 1086 to position 1200. In contrast, analysis of concatenated MLST gene sequences showed no significant regions probable for recombination.

Phylogeny of *eibG*-positive STEC. *eib*G is present in eight STs, and ST33 was predominant (Table 3 and Fig. 4). The minimum spanning tree of all *eibG*-positive STEC strains in comparison to the HUSEC collection (19) (Fig. 5) demonstrates that with a single exception (ST442, which is also present in the HUSEC collection and is a single-locus variant of ST677), the different *eibG*-positive strains were only distantly related to the HUSEC collection, sharing at maximum five of the seven alleles. In some strains of the same ST (e.g., in ST33), various *eibG* alleles with only minor differences (up to 15 nucleotides) were present. In contrast, we found in a subset of *eibG*-positive strains the same *eibG* allele in two different phylogenetically unrelated genomic backgrounds, as shown in Fig. 4: in particular, *eibG* allele 017 was present in strains with ST33 (OR:Hnt [$fliC_{H14}$]) and ST442 (O146:H21), which have only two alleles in common.

Adherence of *eibG*-positive STEC to human and bovine intestinal epithelial cells. On human intestinal epithelial cell line HCT-8, strains of serotype O91:H14/H$^-$ [H14] (ST33), which possess *eibG*-α, formed multiple long chains usually consisting of more than 10 bacteria (Table 4 and Fig. 6A). This typical CLAP was also displayed by an *eibG*-α-harboring STEC strain of serotype OR:H10 belonging to ST745 (Fig. 6D). In contrast, *eibG*-α-positive strains of serotypes O146:H21 (ST442) (Fig.

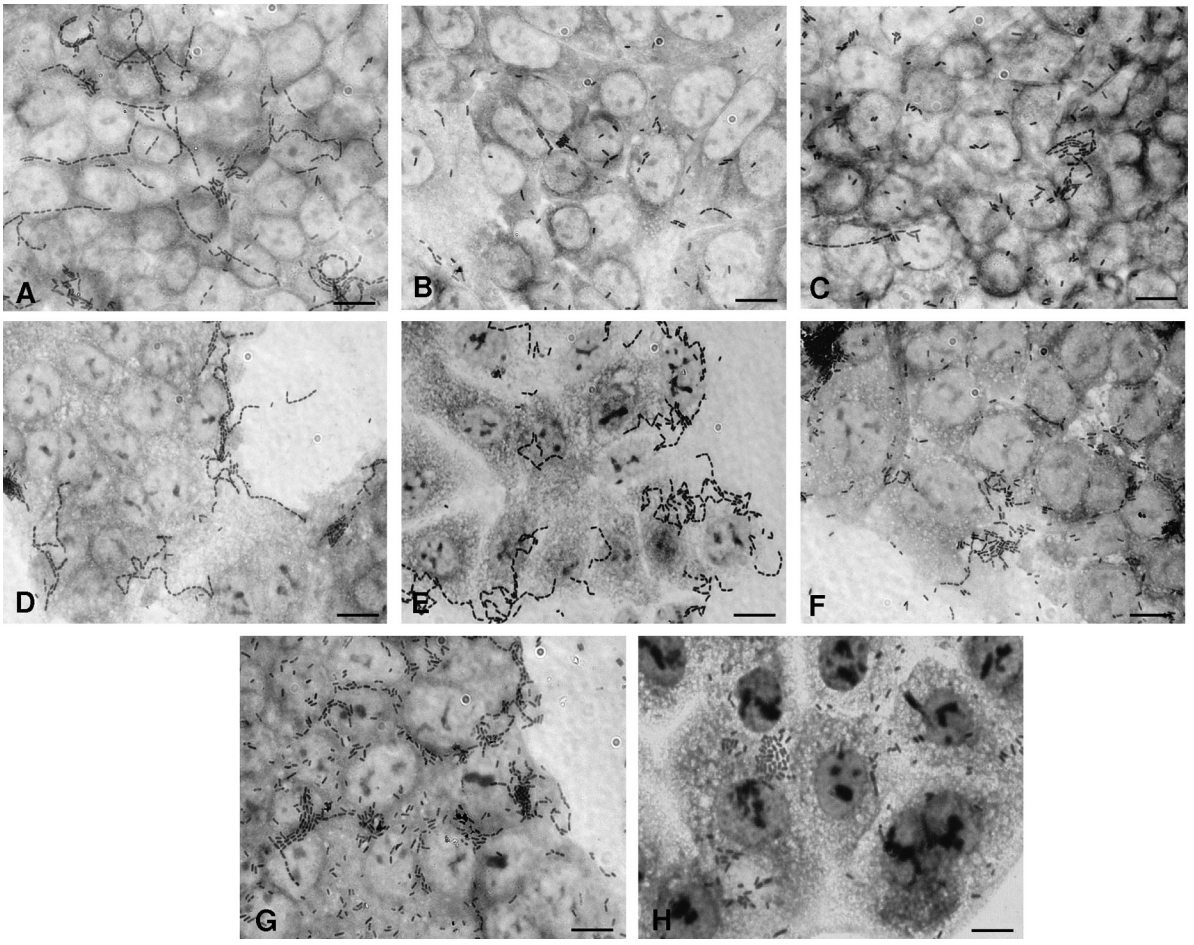

FIG. 6. Patterns of adherence of STEC strains with different EibG subtypes to HCT-8 human intestinal epithelial cells. In panels A to H, the following strains are shown (serotype, ST, and *eibG* subtype are in parentheses): 1809/00 (O91:H$^-$ [H14], ST33, *eibG*-α) (A), 4789/97-1 (O146:H21, ST442, *eibG*-α) (B), 4831/97 (OR:H45, ST656, *eibG*-α) (C), 99-02787 (OR:H10, ST745, *eibG*-α) (D), 06-03233 (O152:H$^-$ [H14], ST13, *eibG*-β) (E), 0519/99 (OR:Hnt, ST753, *eibG*-γ) (F), 0520/99 (Ont:H30, ST753, *eibG*-γ) (G), and 1745/98 (O91:H21, *eibG*-negative control) (H). Bar = 10 μm.

6B) and OR:H45 (ST656) (Fig. 6C) reproducibly formed only short (fewer than 10 bacteria) chains or adhered in small clusters or as single bacteria. An atypical CLAP, i.e., mostly short chains, often organized in parallel, was also displayed by each of the two strains containing *eibG*-γ (Fig. 6F and G). The only STEC strain containing *eibG*-β expressed a typical CLAP with multiple long chains (Fig. 6E). The adherence phenotype was independent of the presence of mannose. These data suggest that the ability of *eibG*-harboring STEC strains to express the typical CLAP, described previously for STEC O91 (17), may depend on the *eibG* subtype (or its particular allele) and/or on the genetic background of the strain (and probably also on the presence of other adhesins).

To determine if the origin of the intestinal epithelial cells can influence the adherence phenotypes, the strains with different *eibG* alleles were also tested for adherence to bovine intestinal epithelial cells (line FKD-R 971) (Fig. 7). These cells were selected to mimic the natural niche of STEC in their most frequent reservoir. Similar to results with HCT-8 cells, the *eibG*-α-harboring STEC O91:H14/H$^-$ [H14] (ST33) and the *eibG*-β-harboring STEC produced typical CLAP (Fig. 7A and C, respectively), whereas the *eibG*-α-positive strain O146:H21 (ST442) and the *eibG*-γ-containing strain produced an atypical CLAP (Fig. 7B and D, respectively). This suggests that the adherence phenotypes of STEC with different *eibG* alleles are independent of the species origin of the intestinal epithelial cells.

Expression of EibG-α, EibG-β, and EibG-γ in STEC strains. To determine if the failure of STEC harboring *eibG*-γ to produce typical CLAP might be a result of the lack of expression of the EibG protein, we performed fluorescence staining of representative STEC harboring *eibG*-α, *eibG*-β, and *eibG*-γ with Alexa 488-labeled human IgG Fc fragment (Fig. 8). Bright peripheral fluorescence suggesting the presence of each respective EibG protein on the bacterial surface was observed in all strains with the different *eibG* subtypes (Fig. 8A to C) but not in an *eibG*-negative STEC O91:H21 strain used as a negative control (Fig. 8D). The specificity of the fluorescence reaction was confirmed by the ability of unlabeled IgG Fc fragment to block bacterial binding of the Alexa 488-labeled IgG Fc fragment (Fig. 8E). Interestingly, bacteria directly from LB broth cultures, which were used in these experiments, already displayed a tendency to form longer (strains expressing EibG-α and EibG-β) or shorter (strains expressing EibG-γ)

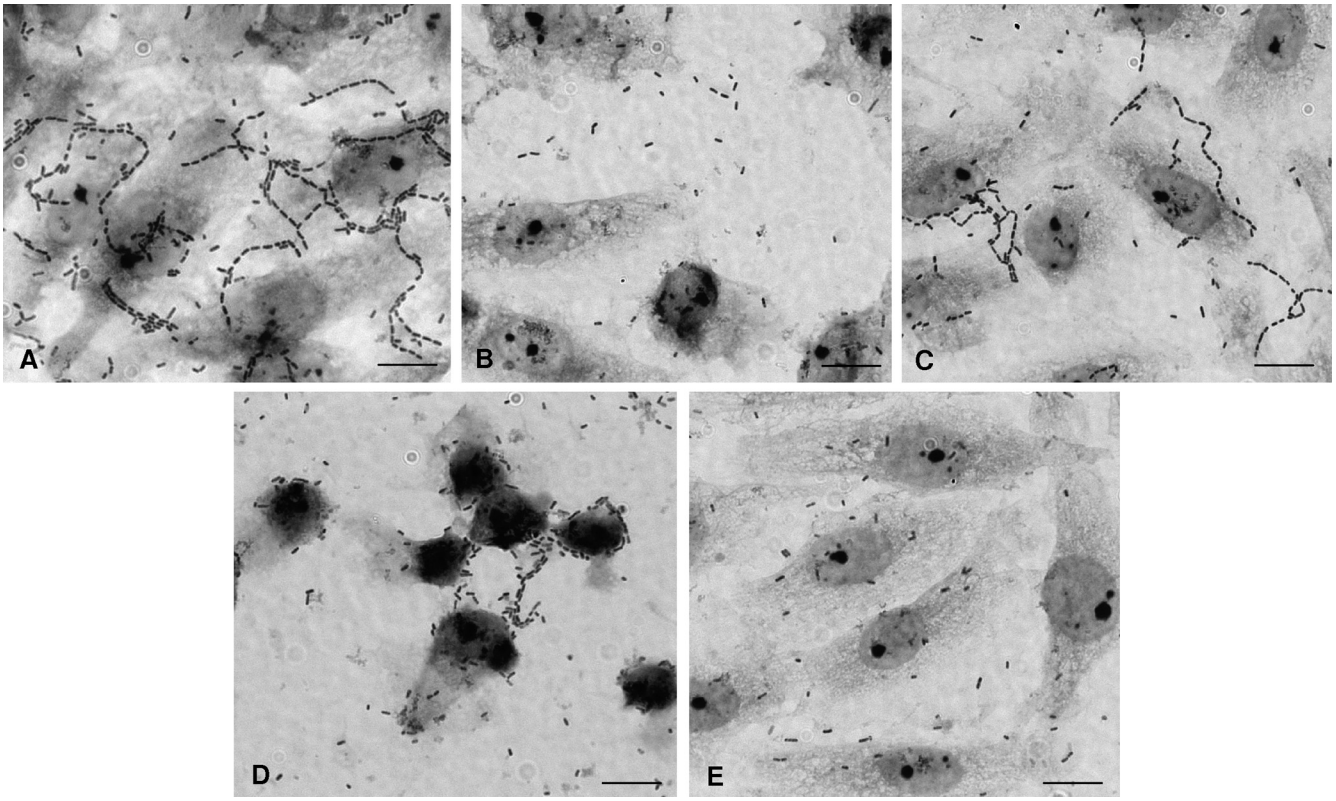

FIG. 7. Patterns of adherence of STEC strains with different EibG subtypes to FDK-R 971 bovine intestinal epithelial cells. In panels A to E, the following strains are shown (serotype, ST, and *eibG* subtype are in parentheses): 7140/96 (O91:H$^-$ [H14], ST33, *eibG*-α) (A), 4789/97-1 (O146:H21, ST442, *eibG*-α) (B), 06-03233 (O152:H$^-$ [H14], ST13, *eibG*-β) (C), 0520/99 (Ont:H30, ST753, *eibG*-γ) (D), and 1745/98 (O91:H21, *eibG*-negative control) (E). Bar = 20 μm.

chains, suggesting that contact with the epithelial cells is not necessary for the expression of the CLAP phenotype. Instead, this observation suggests that EibG might be involved in chain formation during bacterial growth.

Adherence phenotypes of clones harboring different *eibG* subtypes. To determine the role of the host strain background in the different CLAP phenotypes displayed by STEC strains harboring the different *eibG* subtypes, we cloned whole genes encoding EibG-α, EibG-β, and EibG-γ from these STEC strains into the *E. coli* BL21(DE3) host strain (Table 2). The CLAP phenotypes of the clones (Fig. 9) closely resembled those displayed by the respective parental STEC strains (Fig. 6). Specifically, clones B-1-10 and B-20-1, which contain *eibG*-α from STEC O91:H14 and *eibG*-β, respectively, produced long chains (typical CLAP) (Fig. 9A and C), whereas clones B-10-9 and B-18-2, harboring *eibG*-α from STEC O146:H21 and *eibG*-γ, respectively, produced mostly short chains and clusters (atypical CLAP) (Fig. 9B and D). These data suggest that the *eibG* subtype itself (and its particular allele in the case of *eibG*-α), rather than the host strain background, is responsible for the different adherence phenotypes displayed by STEC strains harboring the respective *eibG* genes. *eibG* expression in the clones was confirmed by their ability to bind Alexa 488-labeled human IgG Fc fragment to their surface (data not shown).

DISCUSSION

We found *eibG* to be strongly associated with *eae*-negative STEC strains of multiple serotypes, thereby extending the original observation of Lu et al. (17), who found *eibG* in STEC strains of serogroup O91. We also demonstrated that only one of the four lineages of STEC O91 associated with human disease in Germany (3, 5, 39, 40), specifically STEC O91:H14/H$^-$/Hnt [H14], contains *eibG*. The other three O91 serotypes isolated from patients, including O91:H8, O91:H10, and O91:H21 (5, 21), lack this gene. This differential presence of *eibG* adds to the previously identified differences in the spectrum of putative virulence loci between members of the STEC O91 serogroup (5). Moreover, in contrast to other *eib* genes (29, 30), *eibG* is absent from all 72 ECOR strains.

Second, we have demonstrated structural variations in the *eibG* genes. In addition to the originally described *eibG* sequence (17) (GenBank accession number AB255744) corresponding to the allele *eibG* 001 in our study, we identified 20 additional *eibG* alleles that share 88.11% to nearly 100% homology with the reference *eibG* sequence. Not only did all *eibG* alleles contain at least one nonsynonymous nucleotide substitution, but nearly all also contained more nonsynonymous than synonymous nucleotide substitutions, indicating a probable selection for diversification. This structural variability in the *eibG* gene, not recognized previously, allowed us to designate three

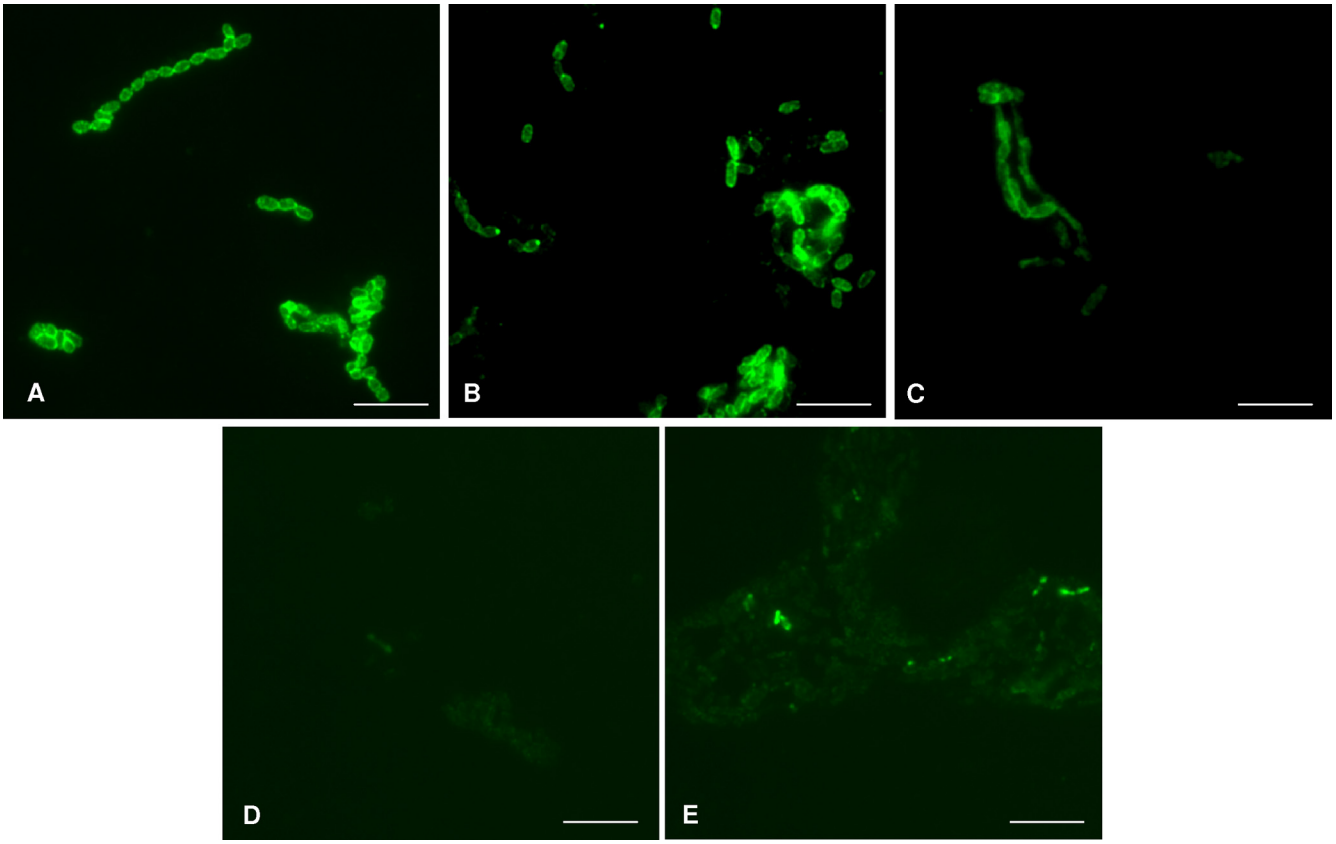

FIG. 8. Expression of different EibG protein subtypes in STEC, demonstrated by fluorescence staining of strains harboring *eibG*-α, *eibG*-β, and *eibG*-γ with Alexa 488-labeled human IgG Fc fragment. In panels A to C, the following strains are shown (serotype, ST, and *eibG* subtype are in parentheses): 99-02787 (OR:H10, ST745, *eibG*-α) (A), 06-03233 (O152:H$^-$ [H14], ST13, *eibG*-β) (B),and 0520/99 (Ont:H30, ST753, *eibG*-γ) (C). Panel D shows the *eibG*-negative STEC O91:H21 strain 1745/98 (negative control), and panel E shows strain 99-02787 (OR:H10, ST745, *eibG*-α), which was preincubated with nonlabeled human IgG Fc fragment before the fluorescence staining. Bar = 10 μm.

subtypes (*eibG*-α, -β, and -γ), which substantially differ in their predicted amino acid structures. Because EibG might be involved in the host-pathogen interaction (17), this diversification might reflect adaptation of the pathogen to the environment of the host (32). Further testing of the null hypothesis ($d_N = d_S$) underlined the presence of positive selection within *eibG*.

Third, despite the large amino acid sequence diversity of the EibG proteins, where EibG-β and EibG-γ differ from EibG-α by 51 and 61 amino acids, respectively, bacteria expressing the different EibG subtypes display the chain-like phenotype, though the chain length is different. This is consistent with observations for other STEC virulence factors, e.g., Stx and intimin, where different protein variants retain their major function (11, 41). Moreover, the ability of EibG-α, EibG-β, and EibG-γ, respectively, expressed in the same genomic background [*E. coli* BL21(DE3)] to mediate CLAP phenotypes identical to those displayed by the respective parental STEC strains suggests that the EibG subtype itself and not the genomic background of the STEC strain is decisive for the strain's ability to produce typical or atypical CLAP. Notably, the expression already of the chain-like phenotype by bacteria from broth cultures supports the hypothesis that besides contributing to the host cell adherence (17), EibG may also be directly involved in chain formation by growing bacteria and thus in interbacterial contact.

Currently there is limited knowledge about the mechanisms of adherence of STEC to the intestinal epithelium. Most STEC strains isolated from severe human disease, including HUS (i.e., STEC O157:H7, O26:H11, O103:H2, O111:H8, and O145:H28), can tightly attach to the intestinal epithelial cells via intimin (7), which is encoded by *eae* in the LEE pathogenicity island (14). However, some *eae*-negative STEC, in particular serotypes O91:H21 and O113:H21, can also cause HUS (4, 5, 19, 21, 24). We have recently expanded the spectrum of *eae*-negative STEC serotypes associated with HUS by isolating STEC strains of additional serotypes (O55:Hnt, O73:H18, O98:H$^-$, O104:H4, O104:H21, O111:H10, O112:H$^-$, O128:H2, O163:H19, O174:H21, Ont:H21, and Ont:H$^-$) from such patients (these strains are members of the recently established HUSEC collection [19]). The adherence phenotypes of several *eae*-negative STEC strains for cultured cells are diverse (10, 12, 38). One or more adhesin genes, such as *saa*, *iha*, $lpfA_{O26}$, and $lpfA_{O113}$ (8, 23, 31, 35, 37), are present in most *eae*-negative HUSEC strains (19). The EibG protein, encoded by *eibG*, is an additional putative afimbrial adhesin in STEC O91 (17), in particular in serotype O91:H14/H$^-$ [H14], as determined in our study. Notably, as shown previously for STEC O91 (17),

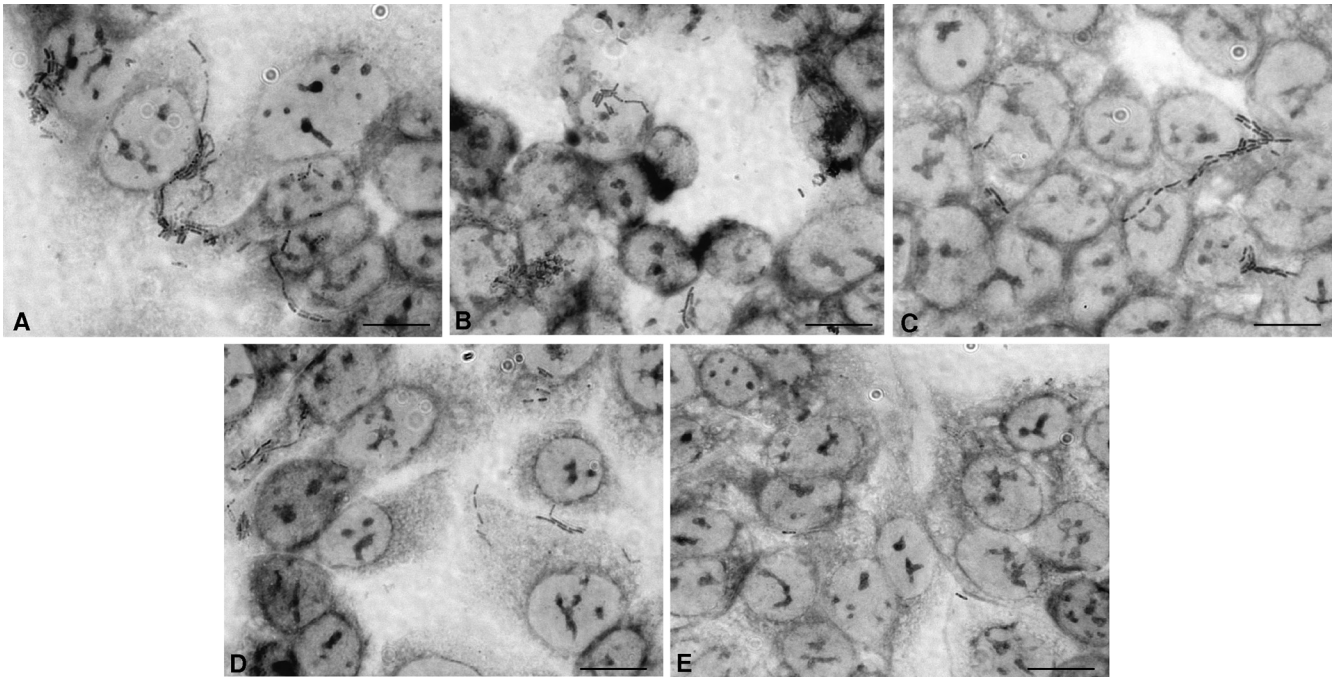

FIG. 9. Adherence phenotypes of clones harboring different *eibG* subtypes on HCT-8 cells. In panels A to E, the following clones are shown (*eibG* subtypes and their origins in parentheses): clone B-1-10 (*eibG*-α from STEC O91:H14, ST33) (A), clone B-10-9 (*eibG*-α from STEC O146:H21, ST442) (B), clone B-20-1 (*eibG*-β from STEC O152:H$^-$ [H14], ST13) (C), clone B-18-2 (*eibG*-γ from STEC Ont:H30, ST753) (D), and *E. coli* BL21(DE3) harboring pGEM-T Easy vector (*eibG*-negative control) (E). Bar = 20 μm.

none of the *eibG*-positive STEC strains of the other serotypes investigated in our study contained *saa*, encoding another common adhesin of *eae*-negative STEC, the STEC autoagglutinating adhesin (Saa). Like Iha, which is also a siderophore receptor (16), EibG might have other roles in addition to its capacity to confer adherence. In contrast to the majority of human-pathogenic STEC strains, which are cleared from the intestinal tract after they have caused disease, STEC O91:H14/H$^-$ can colonize humans for several months (H. Karch, unpublished). It is tempting to speculate that the long-term shedding of STEC O91:H14/H$^-$ (suggesting its persistence in the human intestine) might be associated with the ability of these pathogens to escape the host immune response because of expression of EibG.

We discerned two evolutionary scenarios for *eibG* in STEC. There is a clonal establishment of *eibG* in strains with the same phylogenetic background, i.e., strains sharing identical STs (e.g., all strains of ST33 share very similar *eibG* alleles, differing from the reference sequence in at most 15 nucleotides). However, we also portray evidence for horizontal gene transfer of *eibG* between phylogenetically unrelated STEC strains belonging to different STs, as demonstrated by the presence of eibG 017 in STs 33 and 442 (Table 4 and Fig. 4). Such a scenario is in accordance with reports that *eibG*, in similarity to the other *eib* genes (*eibACEF*) (27), is encoded in the genome of a bacteriophage (17).

In summary, our data extend the knowledge about *eibG* distribution and phylogeny in STEC by demonstrating the presence of *eibG* in different serotypes beyond serogroup O91 and by identifying multiple alleles originating with a putative founder under positive selection by either clonal diversification or horizontal gene transfer. The detected differences in adherence phenotypes warrant further investigations focusing on the host-pathogen interaction to elucidate the role of EibG as a potential virulence factor of STEC.

ACKNOWLEDGMENTS

This study was supported by grants from the Federal Ministry of Education and Research Network Zoonoses (no. 01KI07124 and 01KI07127) and by grants from the Interdisciplinary Center of Clinical Research (IZKF) Münster, no. Me2/023/08 and Müth2/028/10.

We are indebted to Phillip I. Tarr (Washington University School of Medicine, St. Louis, MO) for fruitful discussion during preparation of the manuscript. We also thank Angela Berndt (Friedrich-Loeffler-Institut, Jena, Germany) for help with immunohistochemical staining.

REFERENCES

1. **Aldick, T., M. Bielaszewska, W. Zhang, J. Brockmeyer, H. Schmidt, A. W. Friedrich, K. S. Kim, M. A. Schmidt, and H. Karch.** 2007. Hemolysin from Shiga toxin-negative *Escherichia coli* O26 strains injures microvascular endothelium. Microbes Infect. **9:**282–290.
2. **Bettelheim, K. A.** 2007. The non-O157 Shiga-toxigenic (verocytotoxigenic) *Escherichia coli*; under-rated pathogens. Crit. Rev. Microbiol. **33:**67–87.
3. **Beutin, L., G. Krause, S. Zimmermann, S. Kaulfuss, and K. Gleier.** 2004. Characterization of Shiga toxin-producing *Escherichia coli* strains isolated from human patients in Germany over a 3-year period. J. Clin. Microbiol. **42:**1099–1108.
4. **Bielaszewska, M., A. W. Friedrich, T. Aldick, R. Schurk-Bulgrin, and H. Karch.** 2006. Shiga toxin activatable by intestinal mucus in *Escherichia coli* isolated from humans: predictor for a severe clinical outcome. Clin. Infect. Dis. **43:**1160–1167.
5. **Bielaszewska, M., F. Stoewe, A. Fruth, W. Zhang, R. Prager, J. Brockmeyer, A. Mellmann, H. Karch, and A. W. Friedrich.** 2009. Shiga toxin, cytolethal distending toxin, and hemolysin repertoires in clinical *Escherichia coli* O91 isolates. J. Clin. Microbiol. **47:**2061–2066.
6. **Bridger, P. S., M. Mohr, I. Stamm, J. Fröhlich, W. Föllmann, S. Birkner, H. Metcalfe, D. Werling, G. Baljer, and C. Menge.** 24 April 2010. Primary bovine colonic cells: a model to study strain-specific responses to *Escherichia coli*. Vet. Immunol. Immunopathol. [Epub ahead of print.] doi:10.1016/j.vetimm.2010.04.010.

7. **Donnenberg, M. S., S. Tzipori, M. L. McKee, A. D. O'Brien, J. Alroy, and J. B. Kaper.** 1993. The role of the *eae* gene of enterohemorrhagic *Escherichia coli* in intimate attachment in vitro and in a porcine model. J. Clin. Invest. **92:**1418–1424.
8. **Doughty, S., J. Sloan, V. Bennett-Wood, M. Robertson, R. M. Robins-Browne, and E. L. Hartland.** 2002. Identification of a novel fimbrial gene cluster related to long polar fimbriae in locus of enterocyte effacement-negative strains of enterohemorrhagic *Escherichia coli*. Infect. Immun. **70:**6761–6769.
9. **Dugan, K. A., H. S. Lawrence, D. R. Hares, C. L. Fisher, and B. Budowle.** 2002. An improved method for post-PCR purification for mtDNA sequence analysis. J. Forensic Sci. **47:**811–818.
10. **Dytoc, M. T., A. Ismaili, D. J. Philpott, R. Soni, J. L. Brunton, and P. M. Sherman.** 1994. Distinct binding properties of *eaeA*-negative verocytotoxin-producing *Escherichia coli* of serotype O113:H21. Infect. Immun. **62:**3494–3505.
11. **Friedrich, A. W., M. Bielaszewska, W. Zhang, M. Pulz, T. Kuczius, A. Ammon, and H. Karch.** 2002. *Escherichia coli* harboring Shiga toxin 2 gene variants: frequency and association with clinical symptoms. J. Infect. Dis. **185:**74–84.
12. **Herold, S., J. C. Paton, and A. W. Paton.** 2009. Sab, a novel autotransporter of locus of enterocyte effacement-negative Shiga toxigenic *Escherichia coli* O113:H21, contributes to adherence and biofilm formation. Infect. Immun. **77:**3234–3243.
13. **Johnson, K. E., C. M. Thorpe, and C. L. Sears.** 2006. The emerging clinical importance of non-O157 Shiga toxin-producing *Escherichia coli*. Clin. Infect. Dis. **43:**1587–1595.
14. **Kaper, J. B., J. P. Nataro, and H. L. Mobley.** 2004. Pathogenic *Escherichia coli*. Nat. Rev. Microbiol. **2:**123–140.
15. **Karch, H., P. I. Tarr, and M. Bielaszewska.** 2005. Enterohaemorrhagic *Escherichia coli* in human medicine. Int. J. Med. Microbiol. **295:**405–418.
16. **Léveillé, S., M. Caza, J. R. Johnson, C. Clabots, M. Sabri, and C. M. Dozois.** 2006. Iha from an *Escherichia coli* urinary tract infection outbreak clonal group A strain is expressed in vivo in the mouse urinary tract and functions as a catecholate siderophore receptor. Infect. Immun. **74:**3427–3436.
17. **Lu, Y., S. Iyoda, H. Satou, H. Satou, K. Itoh, T. Saitoh, and H. Watanabe.** 2006. A new immunoglobulin-binding protein, EibG, is responsible for the chain-like adhesion phenotype of locus of enterocyte effacement-negative, Shiga toxin-producing *Escherichia coli*. Infect. Immun. **74:**5747–5755.
18. **Martin, D. P., C. Williamson, and D. Posada.** 2005. RDP2: recombination detection and analysis from sequence alignments. Bioinformatics **21:**260–262.
19. **Mellmann, A., M. Bielaszewska, R. Köck, A. W. Friedrich, A. Fruth, B. Middendorf, D. Harmsen, M. A. Schmidt, and H. Karch.** 2008. Analysis of collection of hemolytic uremic syndrome-associated enterohemorrhagic *Escherichia coli*. Emerg. Infect. Dis. **14:**1287–1290.
20. **Mellmann, A., M. Bielaszewska, L. B. Zimmerhackl, R. Prager, D. Harmsen, H. Tschäpe, and H. Karch.** 2005. Enterohemorrhagic *Escherichia coli* in human infection: in vivo evolution of a bacterial pathogen. Clin. Infect. Dis. **41:**785–792.
21. **Mellmann, A., A. Fruth, A. W. Friedrich, L. H. Wieler, D. Harmsen, D. Werber, B. Middendorf, M. Bielaszewska, and H. Karch.** 2009. Phylogeny and disease association of Shiga toxin-producing *Escherichia coli* O91. Emerg. Infect. Dis. **15:**1474–1477.
22. **Ochman, H., and R. K. Selander.** 1984. Standard reference strains of *Escherichia coli* from natural populations. J. Bacteriol. **157:**690–693.
23. **Paton, A. W., P. Srimanote, M. C. Woodrow, and J. C. Paton.** 2001. Characterization of Saa, a novel autoagglutinating adhesin produced by locus of enterocyte effacement-negative Shiga-toxigenic *Escherichia coli* strains that are virulent for humans. Infect. Immun. **69:**6999–7009.
24. **Paton, A. W., M. C. Woodrow, R. M. Doyle, J. A. Lanser, and J. C. Paton.** 1999. Molecular characterization of a Shiga toxigenic *Escherichia coli* O113:H21 strain lacking *eae* responsible for a cluster of cases of hemolytic-uremic syndrome. J. Clin. Microbiol. **37:**3357–3361.
25. **Perelle, S., F. Dilasser, J. Grout, and P. Fach.** 2004. Detection by 5′-nuclease PCR of Shiga toxin producing *Escherichia coli* O26, O55, O91, O103, O111, O113, O145 and O157:H7, associated with the world's most frequent clinical cases. Mol. Cell Probes **18:**185–192.
26. **Prager, R., U. Strutz, A. Fruth, and H. Tschäpe.** 2003. Subtyping of pathogenic *Escherichia coli* strains using flagellar (H)-antigens: serotyping versus *fliC* polymorphisms. Int. J. Med. Microbiol. **292:**477–486.
27. **Sandt, C. H., J. E. Hopper, and C. W. Hill.** 2002. Activation of prophage *eib* genes for immunoglobulin-binding proteins by genes from the IbrAB genetic island of *Escherichia coli* ECOR-9. J. Bacteriol. **184:**3640–3648.
28. **Sandt, C. H., Y. D. Wang, R. A. Wilson, and C. W. Hill.** 1997. *Escherichia coli* strains with nonimmune immunoglobulin-binding activity. Infect. Immun. **65:**4572–4579.
29. **Sandt, C. H., and C. W. Hill.** 2000. Four different genes responsible for nonimmune immunoglobulin-binding activities within a single strain of *Escherichia coli*. Infect. Immun. **68:**2205–2214.
30. **Sandt, C. H., and C. W. Hill.** 2001. Nonimmune binding of human immunoglobulin A (IgA) and IgG Fc by distinct sequence segments of the EibF cell surface protein of *Escherichia coli*. Infect. Immun. **69:**7293–7303.
31. **Schmidt, H., W. L. Zhang, U. Hemmrich, S. Jelacic, W. Brunder, P. I. Tarr, U. Dobrindt, J. Hacker, and H. Karch.** 2001. Identification and characterization of a novel genomic island integrated at *selC* in locus of enterocyte effacement-negative, Shiga toxin-producing *Escherichia coli*. Infect. Immun. **69:**6863–6873.
32. **Smith, N. H., J. Maynard Smith, and B. G. Spratt.** 1995. Sequence evolution of the *porB* gene of *Neisseria gonorrhoeae* and *Neisseria meningitidis:* evidence of positive Darwinian selection. Mol. Biol. Evol. **12:**363–370.
33. **Sonntag, A., M. Bielaszewska, A. Mellmann, N. Dierksen, P. Schierack, L. H. Wieler, M. A. Schmidt, and H. Karch.** 2005. Shiga toxin 2e-producing *Escherichia coli* isolates from humans and pigs differ in their virulence profiles and interactions with intestinal epithelial cells. Appl. Environ. Microbiol. **71:**8855–8863.
34. **Tamura, K., J. Dudley, M. Nei, and S. Kumar.** 2007. MEGA4: Molecular Evolutionary Genetics Analysis (MEGA) software version 4.0. Mol. Biol. Evol. **24:**1596–1599.
35. **Tarr, P. I., S. S. Bilge, J. C. J. Vary, S. Jelacic, R. L. Habeeb, T. R. Ward, M. R. Baylor, and T. E. Besser.** 2000. Iha: a novel *Escherichia coli* O157:H7 adherence-conferring molecule encoded on a recently acquired chromosomal island of conserved structure. Infect. Immun. **68:**1400–1407.
36. **Tarr, P. I., C. A. Gordon, and W. L. Chandler.** 2005. Shiga-toxin-producing *Escherichia coli* and haemolytic uraemic syndrome. Lancet **365:**1073–1086.
37. **Toma, C., E. Martinez Espinosa, T. Song, E. Miliwebsky, I. Chinen, S. Iyoda, M. Iwanaga, and M. Rivas.** 2004. Distribution of putative adhesins in different seropathotypes of Shiga toxin-producing *Escherichia coli*. J. Clin. Microbiol. **42:**4937–4946.
38. **Toma, C., N. Nakasone, E. Miliwebsky, N. Higa, M. Rivas, and T. Suzuki.** 2008. Differential adherence of Shiga toxin-producing *Escherichia coli* harboring *saa* to epithelial cells. Int. J. Med. Microbiol. **298:**571–578.
39. **Werber, D., S. C. Behnke, A. Fruth, R. Merle, S. Menzler, S. Glaser, L. Kreienbrock, R. Prager, H. Tschäpe, P. Roggentin, J. Bockemühl, and A. Ammon.** 2007. Shiga toxin-producing *Escherichia coli* infection in Germany: different risk factors for different age groups. Am. J. Epidemiol. **165:**425–434.
40. **Werber, D., L. Beutin, R. Pichner, K. Stark, and A. Fruth.** 2008. Shiga toxin-producing *Escherichia coli* serogroups in food and patients, Germany. Emerg. Infect. Dis. **14:**1803–1806.
41. **Zhang, W. L., B. Kohler, E. Oswald, L. Beutin, H. Karch, S. Morabito, A. Caprioli, S. Suerbaum, and H. Schmidt.** 2002. Genetic diversity of intimin genes of attaching and effacing *Escherichia coli* strains. J. Clin. Microbiol. **40:**4486–4492.

Editor: S. M. Payne